

# NEUTRON NOISE ANALYSIS OF SIMULATED MECHANICAL AND THERMALHYDRAULIC PERTURBATIONS IN A PWR CORE

L.A Torres<sup>(1)</sup>, D. Chionis<sup>(2)</sup>, C. Montalvo<sup>(1)</sup>, A. Dokhane<sup>(2)</sup> and A. García-Berrocal<sup>(1)</sup>

(1) Energy and Fuels department, Technical University of Madrid (UPM)

Ríos Rosas 21, 28003 Madrid, Spain

(2) Paul Scherrer Institut, Laboratory for Reactor Physics and Thermal-Hydraulics, CH-

5232 Villigen PSI, Switzerland

## ABSTRACT

KWU-PWR plants show a high level of neutron noise that usually represents added problems in their operation. The frequency region of interest is below 1 Hz, so that thermohydraulic oscillations seem to be one of the main reasons behind. Nevertheless, recently, the neutron noise has experienced an increase in its normalized root mean square that coincide in time with the introduction of a new design of fuel assembly. This fact points out that there should be some relationship between neutron noise spectral characteristics and fuel assemblies' performance. In order to advance in understanding this phenomenon, the transient nodal code SIMULATE-3K (S3K) has been used to simulate mechanical vibrations of fuel assemblies and thermohydraulic oscillations of the core inlet flow. The simulated results obtained are neutron detectors signals which are analysed with noise analysis techniques and compared to real data.

### **Keywords:**

Noise analysis, neutron noise, Simulate 3K, mechanical perturbations, thermalhydraulic perturbations

## 1. INTRODUCTION

In a region of the reactor, neutron noise can be defined as to the series of neutron flux fluctuations around the mean value which is considered stationary in a certain time period [1]. It carries information about the processes that are taking place in the reactor [2-6]. These fluctuations are detected by a series of in-core and ex-core sensors that are part of the reactor instrumentation.

The neutron noise phenomenon occurs in all types of fission reactors. In the particular case of KWU-PWR (German design) high values of neutron noise have been observed since the beginning of their operation [2,7-11]. In spite of high neutron flux fluctuation does not represent problems for the safety of the installation, this type of plants has to take measurements in order to monitor the neutron noise levels. In the past, filters were installed at the very beginning of their operation [12] so as to avoid the unnecessary action of the limitation system every time the neutron noise exceeds a certain threshold; the limitations in neutron noise maximum value are set by the corresponding Safety Authority. In some cases, in the first years of operation, KWU-PWR had to make automatic power reductions [9,12].

In a KWU-PWR, in the neutron noise power spectral density, the low frequency band, below 1 Hz, makes up more than 95 % of the total signal, and it decreases exponentially with frequency [13]. This region has been studied for surveillance purposes and for detecting core flow anomalies in several papers [10,11,14,15]. This frequency range coincides with the frequency of maximum response to thermohydraulic oscillations, the heat transfer processes as well as the moderator temperature coefficient (MTC) feedback [2,3,16,17]. The relationship of neutron noise behaviour and thermohydraulic oscillations has been addressed in several studies, where simulations of scenarios that consider flow and temperature oscillations have been analysed ([18-20]).

However, recently there has been an increase in the neutron noise normalized root mean square (NRMS) that coincides over time with the introduction of a new type of fuel elements, leading again to automatic power reductions [21,22]. This fact points out to the fuel elements as a possible direct cause of this evolution, as well as its relationship with the neutron noise [23]. In [24], the authors showed correlations between the increased neutron noise level and the change in the fuel elements eigenfrequency. In this sense, the interest arises to study simulations where mechanical vibrations of fuel elements are considered.

In order to understand the phenomenon, the transient code simulator S3K is used to simulate certain scenarios in which, on the one hand, mechanical perturbations and on the other hand, thermohydraulic oscillations are supposed to occur at the entrance of the core. The results from the simulations are analysed with noise analysis techniques and compared to KWU-PWR plant data.

The cross-feedback between the mechanical and thermohydraulic disturbances existing in the core complicates the identification of the origin of the neutron noise. When we analyse the simulated scenarios, we can observe how the spectral characteristics, to a certain extent, seem to be associated separately to different causes. In this sense, the results of this work seem to indicate the spectral features of the neutron noise as a consequence of both mechanical perturbations and thermohydraulic fluctuations.

## 2. NEUTRON NOISE PHENOMENOLOGY

The neutron flux density at any region of the core, as recorded by neutron detectors, it is expected to have a constant value over time under steady-state operating conditions. Nevertheless, if the measurements are sufficiently sensitive, we can record very small fluctuations around the signal mean value. These fluctuations are referred as signal noise and it is also observed in various control parameters such as pressure, flow, temperature and mechanical vibrations.

The neutron noise measured in the reactor can be detected by a series of sensors located inside and outside the core; namely the in-core and ex-core neutron detectors. Signal analysis techniques have demonstrate that the neutron noise signals are correlated in both time and space, at a certain extent, even they are random in nature.

It is known that the changes in the mean value in the reactor neutronics are linked to the evolution of thermohydraulic and mechanical processes, however, the cross and simultaneous feedbacks between these three processes make the identification of their relationships a quite complex problem, and consequently, hard to quantify [2,25]. A certain level of correlation is observed among the different processes that transfer these random fluctuations throughout the reactor, i.e., mechanical vibrations and thermohydraulic oscillations.

## 3. NOISE ANALYSIS TECHNIQUES

The results and conclusions obtained in this study are based on the use of analysis tools set, the so-called noise analysis techniques, that have been used for various purposes in nuclear reactor applications [26-28]. Sensor surveillance [29-32] and neutron noise analysis for core diagnostics [33,34] are two of the main applications of noise analysis techniques. Besides recently, and due to the increase in neutron noise levels in certain German and Spanish nuclear reactors, these techniques are being used to comprehend the results from certain simulations [18,20,24]. Therefore, noise analysis techniques allow comparing simulation results with the real data and prove to be necessary to validate the results.

The main tool of noise analysis techniques is based on observing the response of the sensors in the frequency domain through the Fourier transform of the autocorrelation function [35], the so-called auto power spectral density (APSD) defined as:

$$APSD(f) = \int_{-\infty}^{\infty} C_{xx}(\tau) e^{-j2\pi f\tau} d\tau$$

being  $\tau$  the lag used when estimating the autocorrelation function of the sensor output signal  $C_{xx}(\tau)$  which is defined as:

$$C_{xx}(\tau) = E[x(\tau)x(t + \tau)]$$

being  $E$  the expected value and  $x(t)$  the sensor output signal. The autocorrelation function can be estimated by considering that the sensor output signal is a discrete time series  $x_i$  with  $N$  points record length and that can be lagged  $k$  times:

$$C_k = \frac{1}{N-k} \sum_{i=1}^{N-k} x_i x_{i+k} \quad k = 1, 2 \dots N-1$$

Analogously, for two variables, we can calculate the cross power spectrum density (CPSD) through the Fourier transform of the cross correlation between both signals:

$$CPSD(f) = \int_{-\infty}^{\infty} C_{xy}(\tau) e^{-j2\pi f\tau} d\tau$$

being  $C_{xy}$  the cross correlation between signal  $x$  and  $y$ , defined as:

$$C_{xy}(\tau) = E[x(\tau)y(t+\tau)]$$

These tools can be used to calculate the two signals' coherence (COH) and their phase (PHASE), defined as:

$$COH^2(f) = \frac{|CPSD(f)|^2}{APSD_1(f)APSD_2(f)}$$

$$PHASE(f) = \arctg \frac{\text{Im}|CPSD(f)|}{\text{Re}|CPSD(f)|}$$

The coherence takes values between 0 and 1. A zero coherence ( $COH^2 \approx 0$ ) for some considered frequency means that the two analyzed signals' contents are not correlated, or its correlation is very low. A value  $COH^2 \approx 1$  means that the two considered signals' contents are highly correlated. The PHASE is defined as the phase angle between the correlated signals

However, the estimated APSDs based on plant data are not always very smooth, and it is preferable to fit the APSDs to a nonlinear function in order to estimate more accurately certain parameters, such as the response time, eigenfrequencies, amplitudes, damping, etc. Consequently, building an autoregressive (AR) model is an often used solution for this purpose [31,36]. The AR coefficients  $a_k$  are derived by solving the Yule Walker equation:

$$C_j = \sum_{k=1}^n a_k \cdot C_{j-k} \quad j = 0 \dots N$$

being  $n$  the AR model order and  $C_j$  the values of the estimated correlation function at the different  $j$  lags. The expression for the AR model is:

$$x_i = \sum_{k=1}^n x_{i-k} a_k + \varepsilon_i \quad i = 0 \dots N$$

Being  $a_k$  the autoregressive coefficients of the AR model,  $\varepsilon_i$  the input driven white noise and  $x_i$  the output sensor signal. The AR model order can be inferred with the Akaike Information Criterion (AIC) [37].

#### 4. PREPARATION OF SIMULATED SCENARIOS

Neutron noise is a rather complex phenomenon depending on various stochastic processes taking place inherently in any nuclear reactor. These stochastic processes can be related, among others, to fluctuation of thermal-hydraulic parameters (e.g. inlet coolant temperature and flow, etc.) or to vibration of fuel assemblies and structural materials. Modelling these stochastic processes with advanced full core simulators is beneficial for the systematic analysis of the neutron noise characteristics. In this paper, the PWR core developed in the framework of the OECD/NEA transient benchmark [38] has been used to simulate stochastic perturbations and assess their impact on neutron noise phenomenology. This core has been modelled using the CASMO5/SIMULATE3 code sequence and the dynamic simulations have been performed through the S3K code. S3K is a transient nodal simulator including coupled neutronic and thermal-hydraulic capabilities.

##### Thermal-hydraulic parameters fluctuations

In the framework of this project, the inlet coolant flow and temperature are modelled to fluctuate randomly over time using the S3K code. The user can impose time-dependent fluctuations of these parameters using the input cards HYD.CLB, HYD.CLG, HYD.CLT, and HYD.CLW, as already presented in [19]. The analysed core is modelled to have four inlet coolant loops, therefore, the inlet coolant conditions can be perturbed either in a synchronized or in an unsynchronized manner. In other words, the inlet coolant temperature and flow can be fluctuated identically over time among the four coolant loops (synchronized), or randomly (unsynchronized). In addition, with the help of a script written in MATLAB, it is possible to automatize the preparation of the input deck which describes the time-dependent fluctuation of the thermal-hydraulic parameters of interest. With the help of this in-house script, the user can select which parameters are fluctuation, the amplitude of fluctuation, and the dependency between the inlet loops (synchronized or not).

##### Fuel assembly vibrations

One of the latest version of S3K (v2.06.00) offers the capability to mimic the lateral vibration of fuel assemblies in a time-dependent way. This can be achieved by modifying the water gap widths between a fuel assembly which is selected to vibrate and its neighbouring assemblies. The dynamic modification of the water gaps has a direct impact on the time-dependent variation of the homogenized nodal two-group cross-sections allowing the user to model the lateral movement in the x- and/or y-direction. It is to note, that the capability of S3K to properly simulate fuel assemblies vibrations has been showed in [20]. The fuel assembly model in S3K is activated by the KIN.BOW input card. In addition, a set of MATLAB scripts has been developed by PSI in order to automatize the generation of the input file which describes the time-dependent variation of the water gap

widths of the vibrating fuel assemblies. With the help of this complementary set of scripts, the user can control the number and the exact locations of the vibrating fuel assemblies, the amplitude of lateral displacement, the direction of movements (in the x- and/or the y-direction), the type of perturbation (i.e. random over time, or following a sine wave function with a specific nominal frequency), and the dependency of movement between the vibrating fuel assemblies (i.e. identical movement between all the vibrating fuel assemblies; synchronized vibration, or uncorrelated movement; unsynchronized vibration).

## 5. ANALYSED SCENARIOS

This section describes the various analysed scenarios simulated with S3K. The outputs of these simulations are the signals from ex-core and in-core neutron detectors. All the scenarios output include 8 signals from the ex-core detectors placed at 4 different radial locations and at 4 axial levels, and 48 signals from in-core detectors placed at 8 different radial positions and at 6 axial levels. In Figure 1 there is a layout of the core with the locations of both in-core (O5, N12, J2, J6, G10, G14, C4 and B11) and ex-core detectors (S1, S2, S3 and S4). The axial levels are listed from the lower to the higher part, that is, from level 1 (Lv 1) to level 6 (Lv 6).

We can divide the scenarios in two categories; on one hand, scenarios where mechanical vibrations of the fuel elements were analysed, and on the other hand, scenarios where thermohydraulic oscillations were simulated.

The scenarios will be referred in the next sections with the following numbers:

### a) Mechanical vibrations

a.1: Synchronized vibration of the central cluster of 5x5 fuel assemblies only in the x-direction following a white noise signal (random displacement) with displacement amplitude of 1.1 mm. See Figure 1 left side.

a.2: Vibration of a single fuel assembly, located at the position E4, only in the x-direction following a white noise signal (random displacement) with displacement amplitude of 1 mm. See Figure 1 right side.

### b) Thermohydraulic oscillations

b.1 Synchronized fluctuation of inlet coolant temperature between all the four coolant loops. The inlet coolant temperature is randomly fluctuating with amplitude of  $\pm 1^\circ\text{C}$  over the mean value of  $286.7^\circ\text{C}$ .

b.2 Synchronized fluctuation of inlet coolant flow between all the four coolant loops. The inlet coolant flow is randomly fluctuating with amplitude of 1% over the relative flow (100%).

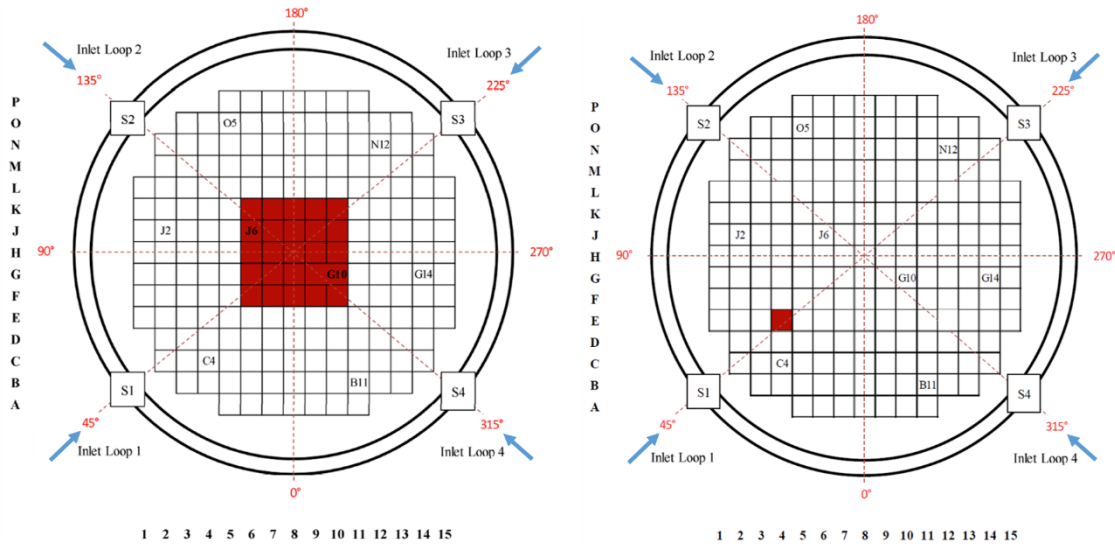


Figure 1: Radial layout of the sensor strings and fuel elements which are vibrating in scenario a.1 and a.2 respectively

## 6. RESULTS FROM THE SIMULATED SCENARIOS

In this section, the results related to the simulations of the described scenarios are presented.

These results are focused in different aspects:

- The intensity of the different detectors response depending on the distance to the perturbation.
- The frequency content of the detectors signals based on the analysis of the APSD.
- The coherence and phase difference between different pair of detectors.
- The comparison of the different scenarios in their distribution of the standard deviation and the NRMS.
- The comparison of the different scenarios with real data.

It is important to mention that in KWU reactors, neutron detectors have very particular spectral characteristics that have not been fully explained. The energy of the signals is four orders of magnitude higher below 1.5 Hz than that of beyond 1.5 Hz. Moreover, out of phase relationship is found between opposite detectors and almost zero phase difference below 2 Hz between lower and upper detectors at the same radial position. In this last noise characteristic, it is possible to see linear phase relationship with a very low slope which indicates that the transport of the phenomenon is very fast [39,40].

### a. Mechanical vibration scenarios

#### *Scenario a.1: Synchronized vibration of the central cluster of 5x5 fuel*

In Figure 2, the APSDs of 8 in-core sensors at the axial level 1 are presented. On the left side, the APSDs from the signals are plotted and on the right side, the APSDs calculated with an AR model from each signal are presented. For comparison purposes, it is more convenient to use an AR model since the APSD gets smoother. The different detectors are located at different distances from the vibrating fuel elements cluster. These distances



are specified in the plot legend. The distances refer to the number of squared nodes apart from the perturbation. It can be observed that the standard deviation decreases with the distance and that the APSDs from detectors at the same distance overlap.

The highest amplitudes of the response are located in the frequency range 0-15 Hz. The lower part of the spectra (i.e. at higher frequencies) does not show a high amplitude, as it is found in real plant data.

It has to be mentioned that the APSDs presented in this section have been normalized in order to ensure that the area below the curve is equal to the signal's variance as it is known from the following equation where the inverse Fourier transform is applied to the APSD [35]:

$$C_{xx}(\tau) = \int_{-\infty}^{\infty} APSD(f) e^{i2\pi f\tau} df \quad \text{for } \tau = 0 \rightarrow C_{xx}(0) = \int_{-\infty}^{\infty} APSD(f) df$$

The autocorrelation function for  $\tau = 0$  is:

$$C_{xx}(\tau = 0) = E[x(\tau)x(t + \tau)] = E[x^2]$$

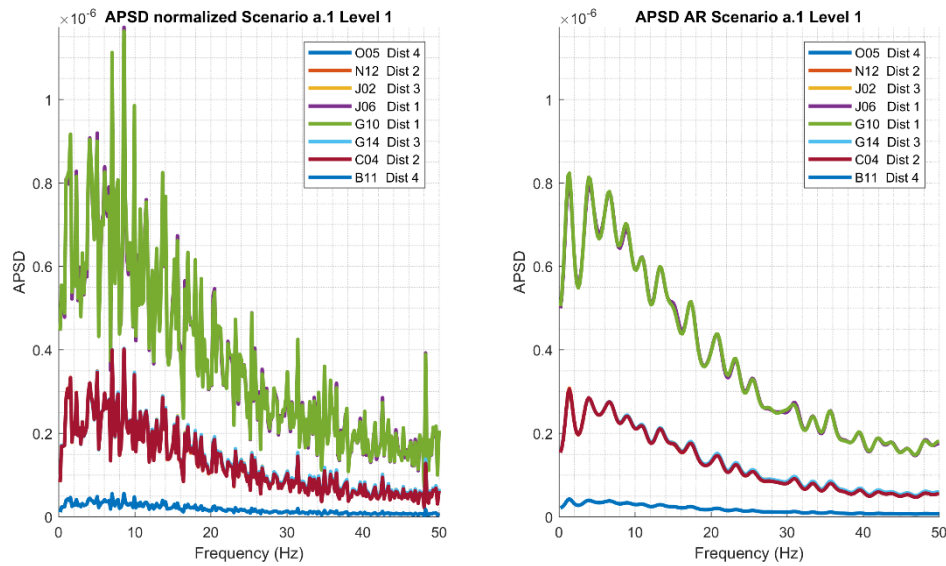


Figure 2: APSDs of 8 In-core sensors at level 1 (left) and AR model of the same in-core sensors (right)

Figure 3 presents the following coherence and phase relationships:

- On the left plot, coherence and phase for all the 8 sensors at the axial level 1, taking as reference the string 4 (J6) sensor.

- On the right plot, coherence and phase for all the axial levels in string 4 (J6), taking as reference the level 1 sensor.

The coherence is one or almost one in all the pairs plotted. Regarding the radial phase relationship, we have a transverse distribution of phase that divides the reactor into two halves clearly differentiated by  $\pm 180$  degrees; the strings (O5, J2, J6, C4) on the left, and the strings (N12, G10, G14, B11) to the right. We must highlight the fact that this out of phase relationship takes place in the whole frequency range.

The phase is null when detector pairs at the same axial level are compared.

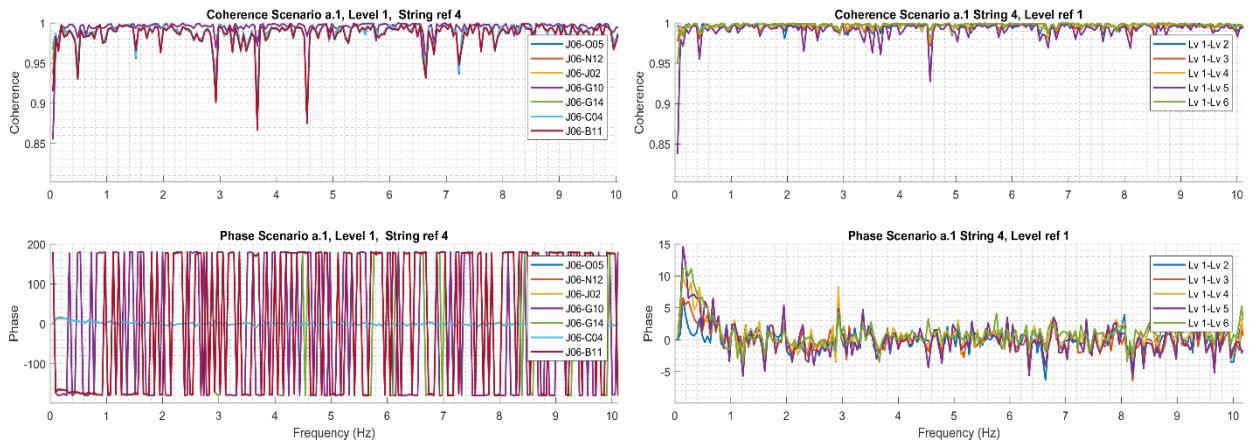


Figure 3: Coherence and phase relationships, radial (left) and axial (right) between incore sensors of the scenario a.1

### Scenario a.2: Vibration of fuel assembly E4

In this scenario we focus on the coherence and radial phase relationships between sensors at the axial level 1, which are shown in Figure 4. In this case we take as reference the string C04, which is the closest to the perturbation source.

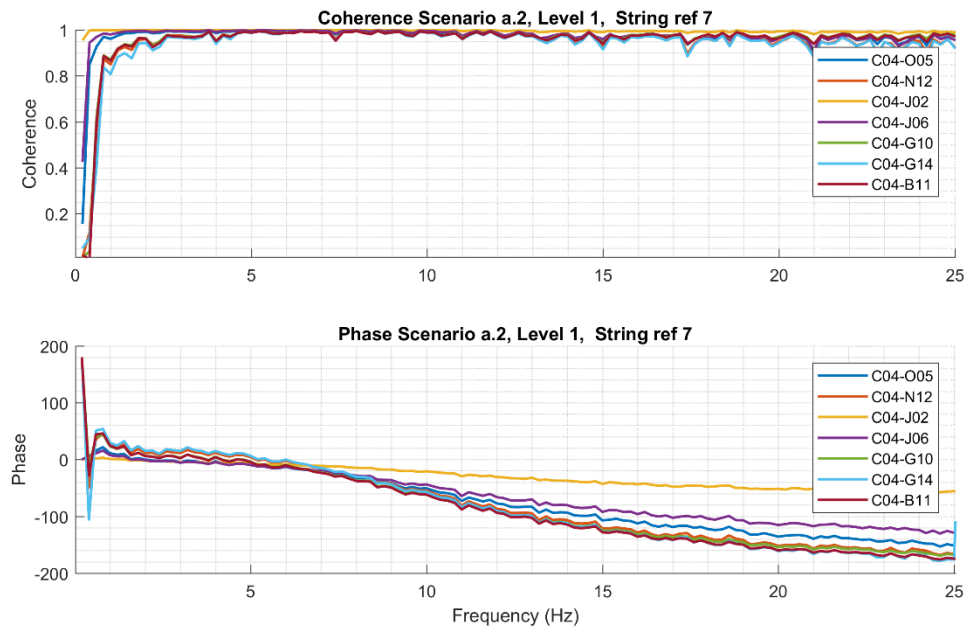


Figure 4: Coherence and radial phase relationships between incore sensors at level 1 with string C4 as reference

As it is observed, we have again almost total coherence between all the analyzed sensors. In the case of phase relationships, the out of phase cannot be appreciated for the frequency range of interest.

In this type of scenario, when a single fuel element is vibrating, the out of phase relationship does not occur while in previous scenario, (clusters of fuel elements) the out of phase extends to the low frequency range (i.e. less than 5Hz), in which thermohydraulic phenomena have a dominant role.

It has to be mentioned that the real data observations are more similar to the scenario a.1; i.e., opposite sensors have an out of phase relationship in all the frequency range [2], as we can see in Figure 5 where coherence and phase from opposite ex-core neutron detectors in a real KWU-PWR are plotted.

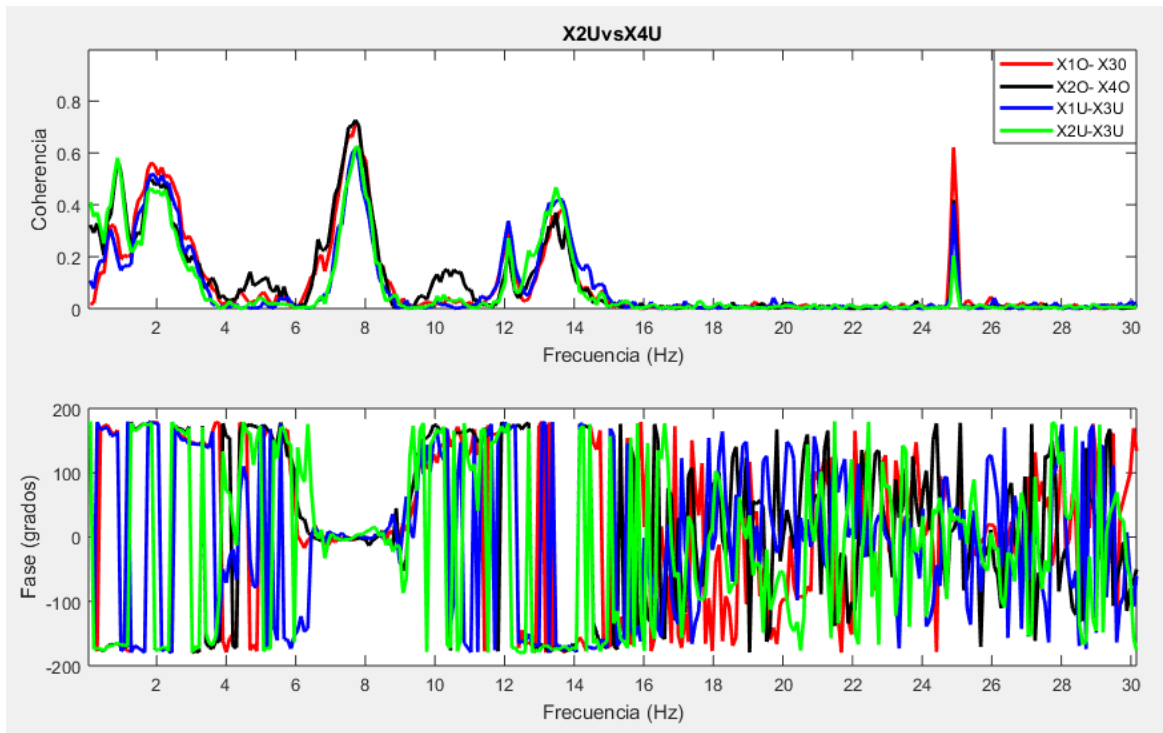


Figure 5: Coherence and radial phase relationships between ex-core opposite detectors of a KWU-PWR plant.

#### b. Thermohydraulic oscillations scenarios

In the thermohydraulic oscillations scenarios; b.1 and b.2, we focus on observing the coherence and axial phase relationships for the six sensors of the string 4 (J06). It is observed in Figure 6, the scenario of fluctuation of the inlet temperature in  $\pm 1$  °C and, in Figure 5 the scenario of fluctuation of the input flow by 1%

As observed in; Figure 6 and Figure 7 for both scenarios, we have a decreasing coherence as the distance from the reference sensor increases, and additionally all the sensors are in phase above 5 Hz.

In this type of scenarios, it is possible to identify, at low frequencies, the characteristic linear phase that indicates the existence of a transport phenomenon. This is not observed in the previous scenarios of fuel elements vibration. The slope of the linear phase is proportional to the transit time according to [2,26] . This means that the higher the slope, the higher the transit time and therefore, the phenomenon of transportation is very slow. Temperature phenomena are characterized, from the point of view of dynamics, by being slow processes, that is, they have big inertia. In this sense, we can see in Figure 6 that the slope of the linear phase in the low frequency range is much higher than the one in Figure 7. This indicates that the flow phenomena are transported much faster than the temperature phenomena. In fact, the phase for in-core detectors at different axial positions in real plant data show a linear phase with a very low slope [41]. Keeping in mind this, the flow perturbations scenarios show more similarities with real plant data than the ones with temperature perturbations.

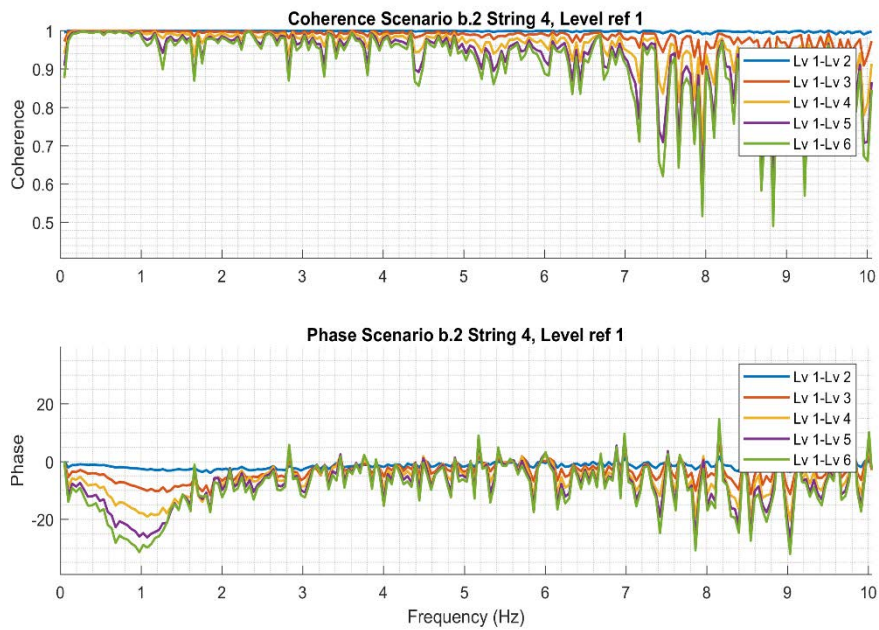


Figure 6: Coherence and phase fluctuation between incore sensors of the flow oscillation scenario

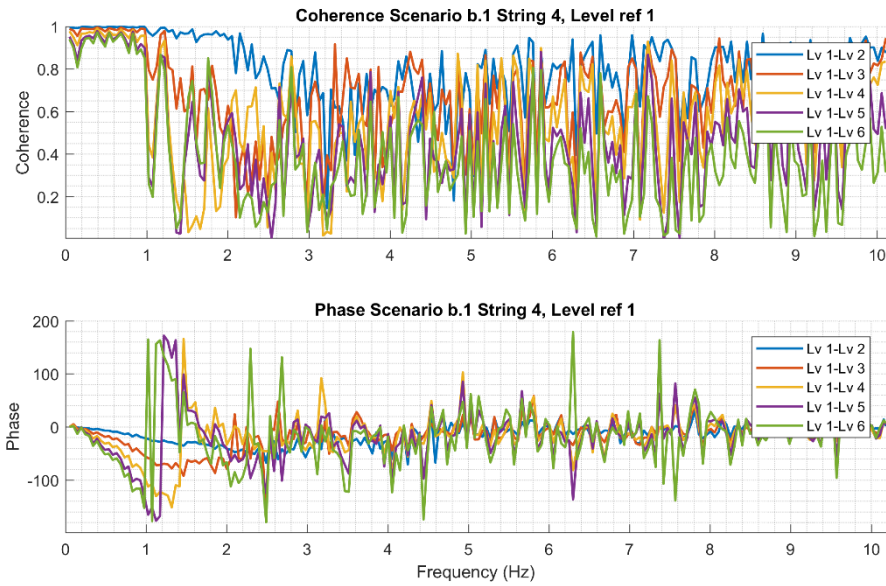


Figure 7: Coherence and phase fluctuation between incore sensors of temperature oscillation scenario

### c. Standard deviation and NRMS of neutron noise

In this subsection, a comparison of the different scenarios based on the values of the signals in terms of standard deviation and NRMS is presented. The standard deviation and NRMS are plotted versus the axial level for two different strings, J02 and J06 (near the edge and in the centre of the core, respectively), and for three simulated scenarios; a.1, central cluster vibration, b.1 and b.2 corresponding to oscillations of coolant inlet temperature and inlet coolant flow rate, respectively.

The standard deviation and NRMS of neutron noise for neutron detector strings J02 and J06 are presented in Figure 8 and Figure 9, respectively. It is observed in both cases that the standard deviation due to the temperature oscillations is the highest of the three cases, followed by the flow case and the one due to vibrations of the fuel elements.

We can see that the profile of the standard deviation and the NRMS in both strings is similar. In [18] the axial profiles obtained resembles the ones regarding flow and temperature perturbations. For flow input perturbations, the NRMS increases with height and for coolant temperature perturbations, it is the opposite, as we can see in Figure 8 and Figure 9 right side. According to [18] temperature fluctuations are supposed to be higher at the bottom since the flow coming from the different loops is not homogenized. In the case of coolant temperature, the exchange of heat along the core reduces fluctuations and makes the differences homogenize. In the case of flow, the nucleate boiling causes a slight increase in the flow fluctuations and consequently a higher NRMS. On the other hand, since the flow perturbations are transported very quickly, the NRMS is not higher at the bottom. These axial profiles coincide to a large extent with the profiles observed in reality, as shown in Figure 10 where data from a string of an in-core detector from a KWU-PWR is plotted.



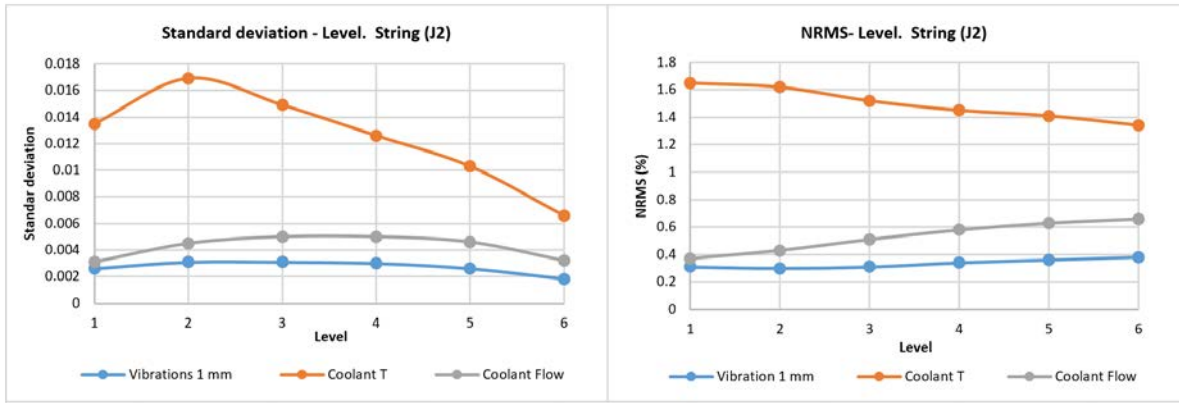


Figure 8: The standard deviation and NRMS versus the axial level in string J02

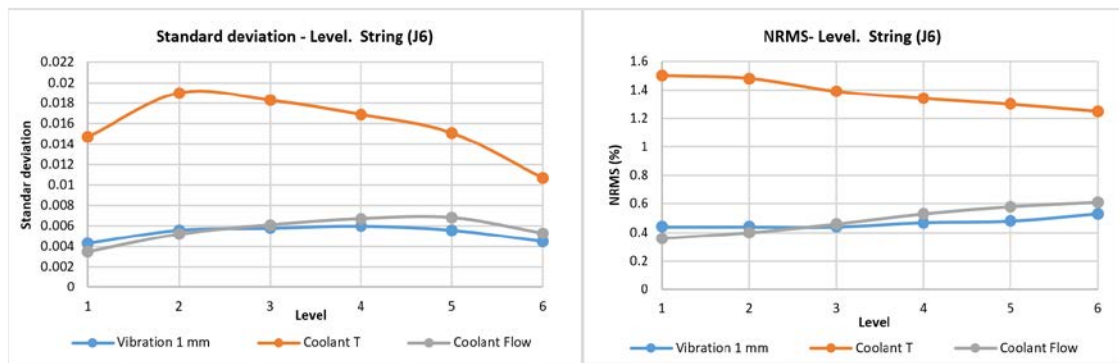


Figure 9: The standard deviation and NRMS versus the axial level in string J06

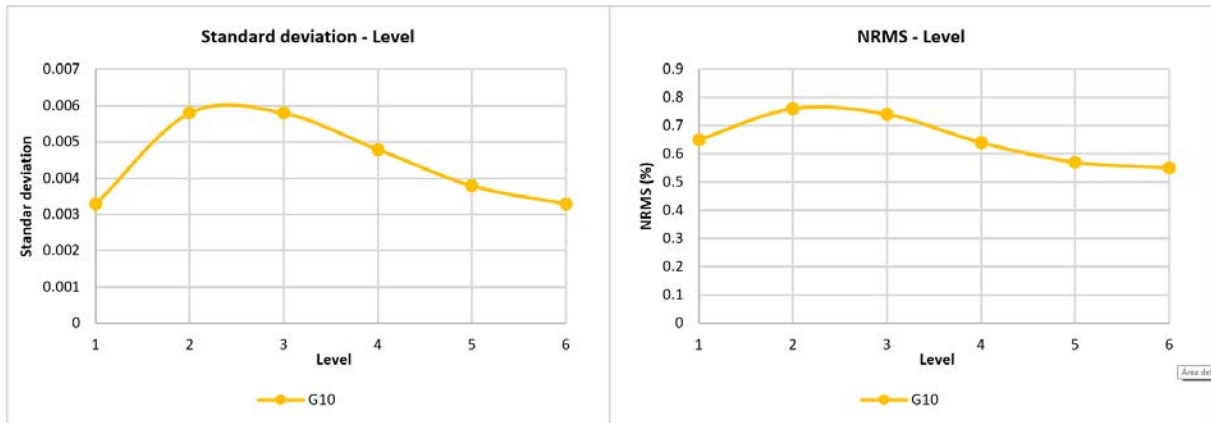


Figure 10: The standard deviation and NRMS versus the axial level in real data

## 7. DISCUSSION

The three types of simulated scenarios considered above, fuel elements mechanical vibrations, oscillations of inlet coolant flow and temperature, seem to produce separately several spectral characteristics observed in neutron noise. Below three characteristics observed in the phenomenology of neutron noise and the possible phenomena associated to their causes will be discussed in detail.

## High transit speed of the transport phenomenon

In real data from KWU plants [2,41], the phase difference relationships between in-core sensors of a same string show a very low slope pointing out the existence of a transport phenomenon with a quite high transit speed, as presented in Figure 11. The real case is similar to what it is observed in the flow oscillations' scenarios. Therefore, this characteristic seems to be linked to flow perturbations at the inlet which unlike the temperature oscillations scenarios, transport along the core almost instantly (see Figure 6 and Figure 7).

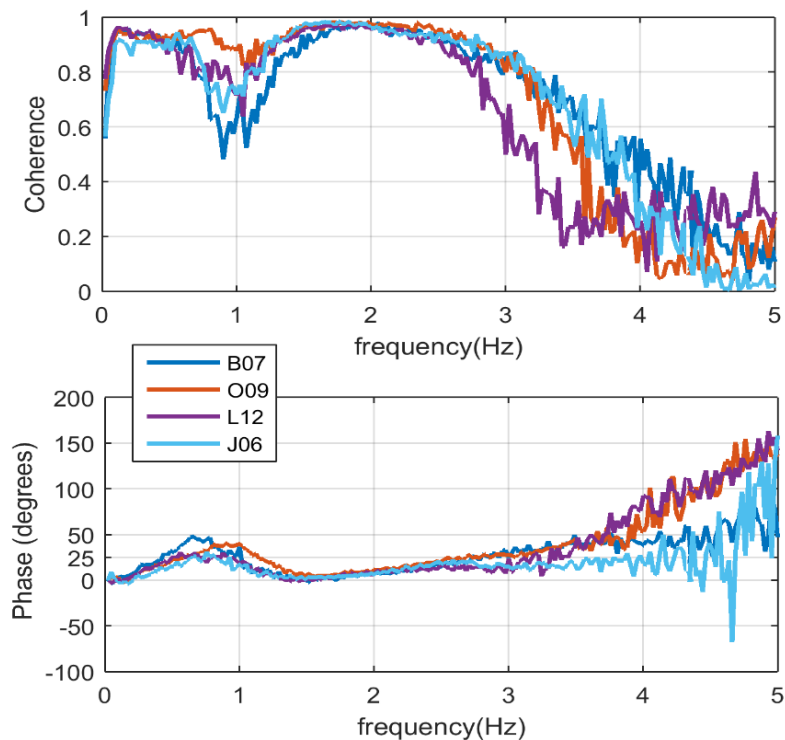


Figure 11: The phase relationships between in-core sensors of a same string in a KWU-PWR

## Response amplitude at low frequencies, below 1 Hz

Neutron noise has its highest amplitude around 1Hz. This characteristic seems to be related to the thermohydraulic oscillations that are produced in the core and, whose response range is located around 1Hz, as can be seen in Figure 12. We can also point out that the main component of the amplitude seems to be due to temperature oscillations, since this perturbation produces a neutron noise response amplitude four times higher than the flow oscillations and the fuel assemblies' perturbations scenario, as we can also see in Figure 8 and Figure 9.

Besides, the amplitude of neutron noise depends on the amplitude of the imposed perturbation. For example, if more FAs were vibrating or with larger displacement, then the noise amplitude due to this mechanism would be larger. You can easily observe that if you compare the noise amplitude in the frequency domain between scenarios a1 and a2.

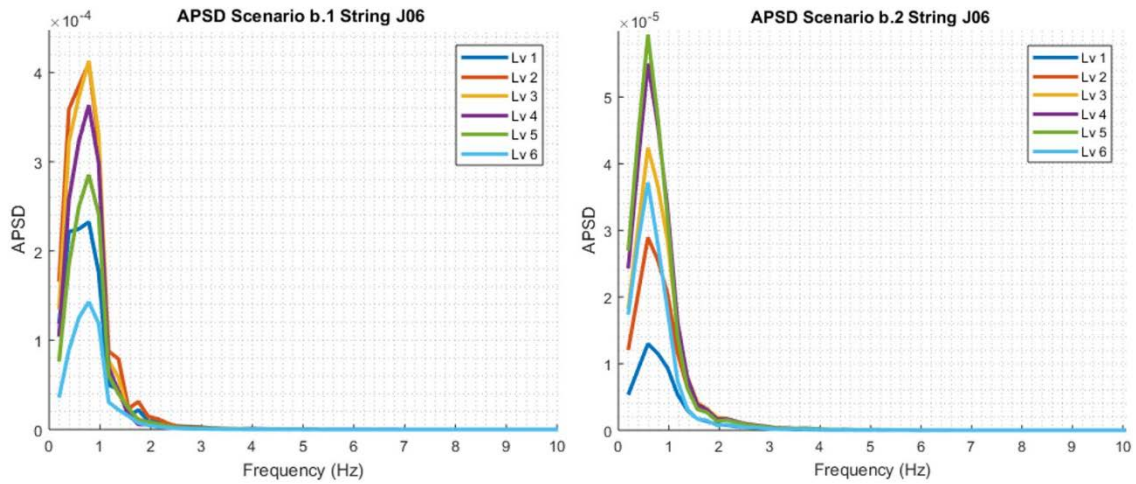


Figure 12: APSDs of thermohydraulic scenarios, temperature and flow oscillations respectively

### Out of phase relationship between opposite detectors

As we have seen, the thermohydraulic oscillations simulations are able to justify and reproduce a big part of the spectral characteristics of the neutron noise, however, these scenarios are not enough to try to explain the out of phase relationship observed between opposite ex-core sensors in KWU reactors. In Figure 5 we saw this phenomenon. For this reason, the mechanical vibrations scenarios are particularly interesting, specifically, the scenario, where a cluster of fuel assemblies is vibrating. This specific scenario leads to an out of phase relationship over the entire frequency range, including the 0-15 Hz band as it is observed in real KWU data [2,42].

The mechanical vibration scenarios with just one fuel assembly do not show the out of phase relationship in the low frequency band, where thermohydraulic phenomena take place. This fact could suggest that in real cases we have clusters of fuel assemblies vibrating in a specific way and causing the characteristic of an out of phase relationship.



## 8. CONCLUSIONS

In this paper several simulation results based on the transient nodal code S3K are analysed from the point of view of the spectral characteristics of the neutron detectors signals. The scenarios analysed were grouped in two types, on the one hand, mechanical perturbation scenarios; in a cluster of fuel assemblies and in only one fuel assembly, and on the other hand, thermohydraulic perturbations; inlet coolant temperature and flow fluctuations.

In the first group of simulated scenarios (mechanical vibrations) we observed how the amplitude of the neutron noise decreases rapidly as the distance from the source of perturbation increases. In-core and ex-core opposite detectors show an out of phase relationship in the entire frequency range when clusters of fuel assemblies are vibrating. In the second group of simulated scenarios (thermohydraulic perturbations) we observed a linear phase difference between upper and lower in-core detectors of the same string which was found to correspond to a transport phenomenon. The transit time calculated from both scenarios show that the flow perturbations are transported much faster than the temperature ones. Regarding the amplitude of the neutron noise, the temperature oscillations cause the highest response values.

Therefore, in real data, the low transit time observed between upper and lower detectors from the same string can be explained if flow perturbations occur at the core inlet. Nevertheless, the high amplitude of the neutron noise below 1 Hz seems to be the result of a temperature perturbation.

As seen in the simulations the spectral characteristics cannot be explained by one single phenomenon. It seems that the amplitude of the neutron noise is due to thermohydraulic oscillations and that the characteristic out of phase relationship in CPSD from opposite detectors is a consequence of fuel assemblies vibrations.

The nature of the spectral characteristics observed in the analysis of the neutron noise illustrates the complexity to define the phenomenon and to identify their possible causes, as well as quantify the relation of each possible cause with the phenomenon itself.

## ACKNOWLEDGEMENTS

The research leading to these results has received funding from the Euratom research and training programme 2014-2018 under grant agreement No 754316.”

## REFERENCES

- [1] Hashemian HM. Maintenance of Process Instrumentation in Nuclear Power Plants. Berlin: Springer, 2006.
- [2] Runkel J. Noise Analysis in Pressurized Water Reactor. PHD Thesis 1987.

- [3] Thie JA. Power Reactor Noise. La Grange Park, IL, USA: American Nuclear Society, 1981.
- [4] Pázsit I, Montalvo-Martin C, Tambouratzis T, Dykin V. Final Report on the Research Project Ringhals Diagnostics and Monitoring Stage 13. 2010.
- [5] Dykin V, Montalvo C, Nylén H, Pázsit I. Ringhals Diagnostics and Monitoring, Final Research Report 2012-2014. 2014;CTH-NT-304/RR-19.
- [6] Pázsit I, Nylén H, Montalvo-Martin C. Refined method for surveillance and diagnostics of the core barrel vibrations of the Ringhals PWRs. 2014.
- [7] Laggiard E, Runkel J. Detection of subcooled boiling in a PWR using noise analysis and calculation of the steam void fraction. *Ann Nucl Energy* 1997;24:49-54.
- [8] Kostic Lea. Estimation of MTC in a PWR as function of neutron noise amplitude. SMORN-6 , Gatlinburg, Tennessee, USA 1991.
- [9] Stegemann D, Runkel J. Experience with vibration monitoring in German PWRs Obrigheim, Grohnde, Brokdorf and Emsland. Proceeding of the SMORN-7 1996.
- [10] Kostic L, Runkel J, Stegemann D. Investigation of the low frequency noise behaviour in a 1350 MW PWR power plant during the first three cycles. Proceeding of IMORN-21 Meeting on Reactor Noise Villigen, Switzerland September 1989.
- [11] Kostic L, Runkel J, Stegemann D. Neutron noise in a power plant near 1Hz. . Proceeding of IMORN-22 Meeting on Reactor Noise Delft Netherlands June 1990.
- [12] Grondey G, Harms R, Kumpf H, Winderl G. Low frequency noise in a PWR and its influence on the normal. operational characteristics of the plant. In-core instrumentation and reactor core assessment Proceedings of Specialist Meeting 1991.
- [13] Seidl M, Kosowski K, Schüler U, Belblidia L. Review of the historic neutron noise behavior in German KWU built PWRs. *Prog Nuclear Energy* 2015;85:668-75.
- [14] Rubiolo PR, Young MY. Characterization of unsteady core flow patterns through noise analysis techniques. *Journal of Power and Energy Systems* 2008;2:435-46.
- [15] Bermejo JA, López A, Ortego A. Study of the spatial dependence of the neutron flux oscillations caused by thermohydraulic fluctuations at the core entrance of a PWR reactor. 40th Annual Meeting of the Spanish Nuclear Society 2014.
- [16] Zylbersztejn F, Tran HN, Pázsit I, Demazière C, Nylén H. On the dependence of the noise amplitude on the correlation length of inlet temperature fluctuations in PWRs. *Ann Nucl Energy* 2013;57:134-41.
- [17] Fry D, March-Leuba J, Sweeney F. Use of neutron noise for diagnosis of in-vessel anomalies in light-water reactors. Use of neutron noise for diagnosis of in-vessel anomalies in light-water reactors 1984;NUREG/CR-3303; ORNL/TM-8774 ON: DE84010431.

- [18] Bermejo J, Montalvo C, Ortego A. On the possible effects contributing to neutron noise variations in KWU-PWR reactor: Modelling with S3K. *Prog Nuclear Energy* 2017;95:1-7.
- [19] Chionis D, Dokhane A, Ferroukhi H, Girardin G, Pautz A. Noise Phenomenology: Part I – Simulation of Stochastic Phenomena with Simulate-3K. . *PHYSOR 2018: Reactor Physics paving the way towards more efficient systems Cancun, Mexico* 2018:1001.
- [20] Chionis D, Dokhane A, Belblidia L, Pecchia M, Girardin G, Ferroukhi H et al. SIMULATE-3K Analyses of Neutron Noise Response to Fuel Assembly Vibrations and Thermal-Hydraulics Parameters Fluctuations. *M&C 2017 - International Conference on Mathematics & Computational Methods Applied to Nuclear Science & Engineering, Jeju, Korea, April 16-20, 2017* 2017.
- [21] RSK/ESK. PWR neutron flux oscillations. Statement (457th meeting on 11.04.2013). 2013.
- [22] Spanish Nuclear Safety Council. Technical Judgement Proposal. Application of 50 revision of the technical especification of operation of Trillo NPP (in Spanish). 2011;CSN/PDT/CNTRI/TRI/1012/129.
- [23] Tran H, Pázsit I, Nylén H. Investigation of the ex-core noise induced by fuel assembly vibrations in the Ringhals-3 PWR. *Ann Nucl Energy* 2015;80:434-46.
- [24] Viebach M, Bernt N, Lange C, Hennig D, Hurtado A. On the influence of dynamical fuel assembly deflections on the neutron noise level. *Prog Nuclear Energy* 2018;104:32-46.
- [25] Pázsit I, Montalvo C, Nylén H, Andersson T, Hernández-Solís A, Cartemo PB. Developments in Core-Barrel Motion Monitoring and Applications to the Ringhals PWR Units. *Nucl Sci Eng* 2016;182:213-27.
- [26] Czibók T, Kiss G, Kiss S, Krinizs K, Végh J. Regular neutron noise diagnostics measurements at the Hungarian Paks NPP. *Prog Nuclear Energy* 2003;43:67-74.
- [27] Hashemian HM. On-line monitoring applications in nuclear power plants. *Prog Nuclear Energy* 2011;53:167-81.
- [28] Ortiz-Villafuerte J, Castillo-Durán R, Alonso G, Calleros-Micheland G. BWR online monitoring system based on noise analysis. *Nucl Eng Des* 2006;236:2394-404.
- [29] Hashemian HM, Jiang J. A practical review of methods for measuring the dynamic characteristics of industrial pressure transmitters. *ISA Trans* 2010;49:2.
- [30] Hashemian HM. Measurement of dynamic Temperatures and Pressures in Nuclear Power Plant. 2011;Phd Thesis, The University of Western Ontario.

- [31] Montalvo C, García-Berrocal A, Balbás M, Blázquez J. AR modelling and DDS for in situ surveillance of capacitive pressure transmitters. Reactor Noise Knowledge Transfer Meeting, Prague 2012.
- [32] Montalvo C, García-Berrocal A, Bermejo J, Queral C. Advanced surveillance of Resistance Temperature Detectors in Nuclear Power Plants. *Ann Nucl Energy* 2014;65:35-40.
- [33] Montalvo C, Pázsit I, Nylén H, Dykin V. First evidence of the pivotal motion ("Tilting Mode") of the Core Barrel in the Ringhals-4 PWR. *PHYSOR 2016 Sun Valley, ID*, May 1–5, 2016.
- [34] Pázsit I, Montalvo C, Nylén H, Andersson T, Hernández-Solís A, Cartemo PB. Developments in Core-Barrel Motion Monitoring and Applications to the Ringhals PWR Units. *Nucl Sci Eng* 2016;182:213-27.
- [35] Newland DE. *An Introduction to Random Vibrations, Spectral and Wavelet Analysis*. : Dover Publications, Incorporated, 2012.
- [36] Blázquez J, Ballestrín J. BWR stability boundary surveillance. *Prog Nuclear Energy* 1995;29:147-52.
- [37] Akaike H. A new look at the statistical model identification. *Automatic Control, IEEE Transactions on* 1974;19:716-23.
- [38] Kozłowski T, Downar TJ. OECD/NEA and US NRC PWR MOX/UO<sub>2</sub> core transient benchmark. Final Specifications, Revision 2003;2.
- [39] Czibók T, Kiss G, Kiss S, Krinizs K, Végh J. Regular neutron noise diagnostics measurements at the Hungarian Paks NPP. *Prog Nuclear Energy* 2003;43:67-74.
- [40] Montalvo C, Ruiz Zapatero M, García-Berrocal A. Estimation of the coolant flow velocity in a PWR: three methods based on noise analysis. *Annual Meeting of the Spanish nuclear Society Valencia* 2014.
- [41] Bermejo JA. Noise analysis in PWR. PHD Thesis 2015.
- [42] Runkel J. ANÁLISIS DE RUIDO EN REACTORES DE AGUA A PRESIÓN. 1987.